Search for techniparticles in e +jets events at D0

V.M. Abazov, B. Abbott, M. Abolins, B.S. Acharya, M. Adams, T. Adams, M. Agelou, S.H. Ahn, M. Ahsan, G.D. Alexeev, et al.

FERMILAB-PUB-06-450-E

Search for techniparticles in e+jets events at D0

V.M. Abazov,[35] B. Abbott,[75] M. Abolins,[65] B.S. Acharya,[28] M. Adams,[51] T. Adams,[49] E. Aguilo,[5] S.H. Ahn,[30] M. Ahsan,[59] G.D. Alexeev,[35] G. Alkhazov,[39] A. Alton,[64,*] G. Alverson,[63] G.A. Alves,[2] M. Anastasoaie,[34] L.S. Ancu,[34] T. Andeen,[53] S. Anderson,[45] B. Andrieu,[16] M.S. Anzelc,[53] Y. Arnoud,[13] M. Arov,[52] A. Askew,[49] B. Åsman,[40] A.C.S. Assis Jesus,[3] O. Atramentov,[49] C. Autermann,[20] C. Avila,[7] C. Ay,[23] F. Badaud,[12] A. Baden,[61] L. Bagby,[52] B. Baldin,[50] D.V. Bandurin,[59] P. Banerjee,[28] S. Banerjee,[28] E. Barberis,[63] P. Bargassa,[80] P. Baringer,[58] C. Barnes,[43] J. Barreto,[2] J.F. Bartlett,[50] U. Bassler,[16] D. Bauer,[43] S. Beale,[5] A. Bean,[58] M. Begalli,[3] M. Begel,[71] C. Belanger-Champagne,[40] L. Bellantoni,[50] A. Bellavance,[67] J.A. Benitez,[65] S.B. Beri,[26] G. Bernardi,[16] R. Bernhard,[22] L. Berntzon,[14] I. Bertram,[42] M. Besançon,[17] R. Beuselinck,[43] V.A. Bezzubov,[38] P.C. Bhat,[50] V. Bhatnagar,[26] M. Binder,[24] C. Biscarat,[19] I. Blackler,[43] G. Blazey,[52] F. Blekman,[43] S. Blessing,[49] D. Bloch,[18] K. Bloom,[67] A. Boehnlein,[50] D. Boline,[62] T.A. Bolton,[59] G. Borissov,[42] K. Bos,[33] T. Bose,[77] A. Brandt,[78] R. Brock,[65] G. Brooijmans,[70] A. Bross,[50] D. Brown,[78] N.J. Buchanan,[49] D. Buchholz,[53] M. Buehler,[81] V. Buescher,[22] S. Burdin,[50] S. Burke,[45] T.H. Burnett,[82] E. Busato,[16] C.P. Buszello,[43] J.M. Butler,[62] P. Calfayan,[24] S. Calvet,[14] J. Cammin,[71] S. Caron,[33] W. Carvalho,[3] B.C.K. Casey,[77] N.M. Cason,[55] H. Castilla-Valdez,[32] S. Chakrabarti,[17] D. Chakraborty,[52] K.M. Chan,[71] A. Chandra,[48] F. Charles,[18] E. Cheu,[45] F. Chevallier,[13] D.K. Cho,[62] S. Choi,[31] B. Choudhary,[27] L. Christofek,[77] D. Claes,[67] B. Clément,[18] C. Clément,[40] Y. Coadou,[5] M. Cooke,[80] W.E. Cooper,[50] M. Corcoran,[80] F. Couderc,[17] M.-C. Cousinou,[14] B. Cox,[44] S. Crépé-Renaudin,[13] D. Cutts,[77] M. Ćwiok,[29] H. da Motta,[2] A. Das,[62] M. Das,[60] B. Davies,[42] G. Davies,[43] K. De,[78] P. de Jong,[33] S.J. de Jong,[34] E. De La Cruz-Burelo,[64] C. De Oliveira Martins,[3] J.D. Degenhardt,[64] F. Déliot,[17] M. Demarteau,[50] R. Demina,[71] D. Denisov,[50] S.P. Denisov,[38] S. Desai,[50] H.T. Diehl,[50] M. Diesburg,[50] M. Doidge,[42] A. Dominguez,[67] H. Dong,[72] L.V. Dudko,[37] L. Duflot,[15] S.R. Dugad,[28] D. Duggan,[49] A. Duperrin,[14] J. Dyer,[65] A. Dyshkant,[52] M. Eads,[67] D. Edmunds,[65] J. Ellison,[48] V.D. Elvira,[50] Y. Enari,[77] S. Eno,[61] P. Ermolov,[37] H. Evans,[54] A. Evdokimov,[36] V.N. Evdokimov,[38] L. Feligioni,[62] A.V. Ferapontov,[59] T. Ferbel,[71] F. Fiedler,[24] F. Filthaut,[34] W. Fisher,[50] H.E. Fisk,[50] M. Ford,[44] M. Fortner,[52] H. Fox,[22] S. Fu,[50] S. Fuess,[50] T. Gadfort,[82] C.F. Galea,[34] E. Gallas,[50] E. Galyaev,[55] C. Garcia,[71] A. Garcia-Bellido,[82] V. Gavrilov,[36] A. Gay,[18] P. Gay,[12] W. Geist,[18] D. Gelé,[18] R. Gelhaus,[48] C.E. Gerber,[51] Y. Gershtein,[49] D. Gillberg,[5] G. Ginther,[71] N. Gollub,[40] B. Gómez,[7] A. Goussiou,[55] P.D. Grannis,[72] H. Greenlee,[50] Z.D. Greenwood,[60] E.M. Gregores,[4] G. Grenier,[19] Ph. Gris,[12] J.-F. Grivaz,[15] A. Grohsjean,[24] S. Grünendahl,[50] M.W. Grünewald,[29] F. Guo,[72] J. Guo,[72] G. Gutierrez,[50] P. Gutierrez,[75] A. Haas,[70] N.J. Hadley,[61] P. Haefner,[24] S. Hagopian,[49] J. Haley,[68] I. Hall,[75] R.E. Hall,[47] L. Han,[6] K. Hanagaki,[50] P. Hansson,[40] K. Harder,[44] A. Harel,[71] R. Harrington,[63] J.M. Hauptman,[57] R. Hauser,[65] J. Hays,[43] T. Hebbeker,[20] D. Hedin,[52] J.G. Hegeman,[33] J.M. Heinmiller,[51] A.P. Heinson,[48] U. Heintz,[62] C. Hensel,[58] K. Herner,[72] G. Hesketh,[63] M.D. Hildreth,[55] R. Hirosky,[81] J.D. Hobbs,[72] B. Hoeneisen,[11] H. Hoeth,[25] M. Hohlfeld,[15] S.J. Hong,[30] R. Hooper,[77] P. Houben,[33] Y. Hu,[72] Z. Hubacek,[9] V. Hynek,[8] I. Iashvili,[69] R. Illingworth,[50] A.S. Ito,[50] S. Jabeen,[62] M. Jaffré,[15] S. Jain,[75] K. Jakobs,[22] C. Jarvis,[61] A. Jenkins,[43] R. Jesik,[43] K. Johns,[45] C. Johnson,[70] M. Johnson,[50] A. Jonckheere,[50] P. Jonsson,[43] A. Juste,[50] D. Käfer,[20] S. Kahn,[73] E. Kajfasz,[14] A.M. Kalinin,[35] J.M. Kalk,[60] J.R. Kalk,[65] S. Kappler,[20] D. Karmanov,[37] J. Kasper,[62] P. Kasper,[50] I. Katsanos,[70] D. Kau,[49] R. Kaur,[26] R. Kehoe,[79] S. Kermiche,[14] N. Khalatyan,[62] A. Khanov,[76] A. Kharchilava,[69] Y.M. Kharzheev,[35] D. Khatidze,[70] H. Kim,[31] T.J. Kim,[30] M.H. Kirby,[34] B. Klima,[50] J.M. Kohli,[26] J.-P. Konrath,[22] M. Kopal,[75] V.M. Korablev,[38] J. Kotcher,[73] B. Kothari,[70] A. Koubarovsky,[37] A.V. Kozelov,[38] D. Krop,[54] A. Kryemadhi,[81] T. Kuhl,[23] A. Kumar,[69] S. Kunori,[61] A. Kupco,[10] T. Kurča,[19] J. Kvita,[8] D. Lam,[55] S. Lammers,[70] G. Landsberg,[77] J. Lazoflores,[49] A.-C. Le Bihan,[18] P. Lebrun,[19] W.M. Lee,[50] A. Leflat,[37] F. Lehner,[41] V. Lesne,[12] J. Leveque,[45] P. Lewis,[43] J. Li,[78] L. Li,[48] Q.Z. Li,[50] S.M. Lietti,[4] J.G.R. Lima,[52] D. Lincoln,[50] J. Linnemann,[65] V.V. Lipaev,[38] R. Lipton,[50] Z. Liu,[5] L. Lobo,[43] A. Lobodenko,[39] M. Lokajicek,[10] A. Lounis,[18] P. Love,[42] H.J. Lubatti,[82] M. Lynker,[55] A.L. Lyon,[50] A.K.A. Maciel,[2] R.J. Madaras,[46] P. Mättig,[25] C. Magass,[20] A. Magerkurth,[64] N. Makovec,[15] P.K. Mal,[55] H.B. Malbouisson,[3] S. Malik,[67] V.L. Malyshev,[35] H.S. Mao,[50] Y. Maravin,[59] R. McCarthy,[72] A. Melnitchouk,[66] A. Mendes,[14] L. Mendoza,[7] P.G. Mercadante,[4] M. Merkin,[37] K.W. Merritt,[50] A. Meyer,[20] J. Meyer,[21] M. Michaut,[17] H. Miettinen,[80] T. Millet,[19] J. Mitrevski,[70] J. Molina,[3] R.K. Mommsen,[44] N.K. Mondal,[28] J. Monk,[44] R.W. Moore,[5] T. Moulik,[58] G.S. Muanza,[19] M. Mulders,[50] M. Mulhearn,[70] O. Mundal,[22] L. Mundim,[3] E. Nagy,[14] M. Naimuddin,[27] M. Narain,[62] N.A. Naumann,[34] H.A. Neal,[64] J.P. Negret,[7]

P. Neustroev,[39] C. Noeding,[22] A. Nomerotski,[50] S.F. Novaes,[4] T. Nunnemann,[24] V. O'Dell,[50] D.C. O'Neil,[5] G. Obrant,[39] C. Ochando,[15] V. Oguri,[3] N. Oliveira,[3] D. Onoprienko,[59] N. Oshima,[50] J. Osta,[55] R. Otec,[9] G.J. Otero y Garzón,[51] M. Owen,[44] P. Padley,[80] M. Pangilinan,[62] N. Parashar,[56] S.-J. Park,[71] S.K. Park,[30] J. Parsons,[70] R. Partridge,[77] N. Parua,[72] A. Patwa,[73] G. Pawloski,[80] P.M. Perea,[48] K. Peters,[44] Y. Peters,[25] P. Pétroff,[15] M. Petteni,[43] R. Piegaia,[1] J. Piper,[65] M.-A. Pleier,[21] P.L.M. Podesta-Lerma,[32] V.M. Podstavkov,[50] Y. Pogorelov,[55] M.-E. Pol,[2] A. Pompoš,[75] B.G. Pope,[65] A.V. Popov,[38] C. Potter,[5] W.L. Prado da Silva,[3] H.B. Prosper,[49] S. Protopopescu,[73] J. Qian,[64] A. Quadt,[21] B. Quinn,[66] M.S. Rangel,[2] K.J. Rani,[28] K. Ranjan,[27] P.N. Ratoff,[42] P. Renkel,[79] S. Reucroft,[63] M. Rijssenbeek,[72] I. Ripp-Baudot,[18] F. Rizatdinova,[76] S. Robinson,[43] R.F. Rodrigues,[3] C. Royon,[17] P. Rubinov,[50] R. Ruchti,[55] G. Sajot,[13] A. Sánchez-Hernández,[32] M.P. Sanders,[16] A. Santoro,[3] G. Savage,[50] L. Sawyer,[60] T. Scanlon,[43] D. Schaile,[24] R.D. Schamberger,[72] Y. Scheglov,[39] H. Schellman,[53] P. Schieferdecker,[24] C. Schmitt,[25] C. Schwanenberger,[44] A. Schwartzman,[68] R. Schwienhorst,[65] J. Sekaric,[49] S. Sengupta,[49] H. Severini,[75] E. Shabalina,[51] M. Shamim,[59] V. Shary,[17] A.A. Shchukin,[38] R.K. Shivpuri,[27] D. Shpakov,[50] V. Siccardi,[18] R.A. Sidwell,[59] V. Simak,[9] V. Sirotenko,[50] P. Skubic,[75] P. Slattery,[71] R.P. Smith,[50] G.R. Snow,[67] J. Snow,[74] S. Snyder,[73] S. Söldner-Rembold,[44] X. Song,[52] L. Sonnenschein,[16] A. Sopczak,[42] M. Sosebee,[78] K. Soustruznik,[8] M. Souza,[2] B. Spurlock,[78] J. Stark,[13] J. Steele,[60] V. Stolin,[36] A. Stone,[51] D.A. Stoyanova,[38] J. Strandberg,[64] S. Strandberg,[40] M.A. Strang,[69] M. Strauss,[75] R. Ströhmer,[24] D. Strom,[53] M. Strovink,[46] L. Stutte,[50] S. Sumowidagdo,[49] P. Svoisky,[55] A. Sznajder,[3] M. Talby,[14] P. Tamburello,[45] W. Taylor,[5] P. Telford,[44] J. Temple,[45] B. Tiller,[24] M. Titov,[22] V.V. Tokmenin,[35] M. Tomoto,[50] T. Toole,[61] I. Torchiani,[22] T. Trefzger,[23] S. Trincaz-Duvoid,[16] D. Tsybychev,[72] B. Tuchming,[17] C. Tully,[68] P.M. Tuts,[70] R. Unalan,[65] L. Uvarov,[39] S. Uvarov,[39] S. Uzunyan,[52] B. Vachon,[5] P.J. van den Berg,[33] B. van Eijk,[35] R. Van Kooten,[54] W.M. van Leeuwen,[33] N. Varelas,[51] E.W. Varnes,[45] A. Vartapetian,[78] I.A. Vasilyev,[38] M. Vaupel,[25] P. Verdier,[19] L.S. Vertogradov,[35] M. Verzocchi,[50] F. Villeneuve-Seguier,[43] P. Vint,[43] J.-R. Vlimant,[16] E. Von Toerne,[59] M. Voutilainen,[67,†] M. Vreeswijk,[33] H.D. Wahl,[49] L. Wang,[61] M.H.L.S Wang,[50] J. Warchol,[55] G. Watts,[82] M. Wayne,[55] G. Weber,[23] M. Weber,[50] H. Weerts,[65] N. Wermes,[21] M. Wetstein,[61] A. White,[78] D. Wicke,[25] G.W. Wilson,[58] S.J. Wimpenny,[48] M. Wobisch,[50] J. Womersley,[50] D.R. Wood,[63] T.R. Wyatt,[44] Y. Xie,[77] S. Yacoob,[53] R. Yamada,[50] M. Yan,[61] T. Yasuda,[50] Y.A. Yatsunenko,[35] K. Yip,[73] H.D. Yoo,[77] S.W. Youn,[53] C. Yu,[13] J. Yu,[78] A. Yurkewicz,[72] A. Zatserklyaniy,[52] C. Zeitnitz,[25] D. Zhang,[50] T. Zhao,[82] B. Zhou,[64] J. Zhu,[72] M. Zielinski,[71] D. Zieminska,[54] A. Zieminski,[54] V. Zutshi,[52] and E.G. Zverev[37]

(DØ Collaboration)

[1] *Universidad de Buenos Aires, Buenos Aires, Argentina*
[2] *LAFEX, Centro Brasileiro de Pesquisas Físicas, Rio de Janeiro, Brazil*
[3] *Universidade do Estado do Rio de Janeiro, Rio de Janeiro, Brazil*
[4] *Instituto de Física Teórica, Universidade Estadual Paulista, São Paulo, Brazil*
[5] *University of Alberta, Edmonton, Alberta, Canada, Simon Fraser University, Burnaby, British Columbia, Canada, York University, Toronto, Ontario, Canada, and McGill University, Montreal, Quebec, Canada*
[6] *University of Science and Technology of China, Hefei, People's Republic of China*
[7] *Universidad de los Andes, Bogotá, Colombia*
[8] *Center for Particle Physics, Charles University, Prague, Czech Republic*
[9] *Czech Technical University, Prague, Czech Republic*
[10] *Center for Particle Physics, Institute of Physics, Academy of Sciences of the Czech Republic, Prague, Czech Republic*
[11] *Universidad San Francisco de Quito, Quito, Ecuador*
[12] *Laboratoire de Physique Corpusculaire, IN2P3-CNRS, Université Blaise Pascal, Clermont-Ferrand, France*
[13] *Laboratoire de Physique Subatomique et de Cosmologie, IN2P3-CNRS, Universite de Grenoble 1, Grenoble, France*
[14] *CPPM, IN2P3-CNRS, Université de la Méditerranée, Marseille, France*
[15] *Laboratoire de l'Accélérateur Linéaire, IN2P3-CNRS et Université Paris-Sud, Orsay, France*
[16] *LPNHE, IN2P3-CNRS, Universités Paris VI and VII, Paris, France*
[17] *DAPNIA/Service de Physique des Particules, CEA, Saclay, France*
[18] *IPHC, IN2P3-CNRS, Université Louis Pasteur, Strasbourg, France, and Université de Haute Alsace, Mulhouse, France*
[19] *Institut de Physique Nucléaire de Lyon, IN2P3-CNRS, Université Claude Bernard, Villeurbanne, France*
[20] *III. Physikalisches Institut A, RWTH Aachen, Aachen, Germany*
[21] *Physikalisches Institut, Universität Bonn, Bonn, Germany*
[22] *Physikalisches Institut, Universität Freiburg, Freiburg, Germany*
[23] *Institut für Physik, Universität Mainz, Mainz, Germany*
[24] *Ludwig-Maximilians-Universität München, München, Germany*
[25] *Fachbereich Physik, University of Wuppertal, Wuppertal, Germany*
[26] *Panjab University, Chandigarh, India*
[27] *Delhi University, Delhi, India*

[28] *Tata Institute of Fundamental Research, Mumbai, India*
[29] *University College Dublin, Dublin, Ireland*
[30] *Korea Detector Laboratory, Korea University, Seoul, Korea*
[31] *SungKyunKwan University, Suwon, Korea*
[32] *CINVESTAV, Mexico City, Mexico*
[33] *FOM-Institute NIKHEF and University of Amsterdam/NIKHEF, Amsterdam, The Netherlands*
[34] *Radboud University Nijmegen/NIKHEF, Nijmegen, The Netherlands*
[35] *Joint Institute for Nuclear Research, Dubna, Russia*
[36] *Institute for Theoretical and Experimental Physics, Moscow, Russia*
[37] *Moscow State University, Moscow, Russia*
[38] *Institute for High Energy Physics, Protvino, Russia*
[39] *Petersburg Nuclear Physics Institute, St. Petersburg, Russia*
[40] *Lund University, Lund, Sweden, Royal Institute of Technology and Stockholm University, Stockholm, Sweden, and Uppsala University, Uppsala, Sweden*
[41] *Physik Institut der Universität Zürich, Zürich, Switzerland*
[42] *Lancaster University, Lancaster, United Kingdom*
[43] *Imperial College, London, United Kingdom*
[44] *University of Manchester, Manchester, United Kingdom*
[45] *University of Arizona, Tucson, Arizona 85721, USA*
[46] *Lawrence Berkeley National Laboratory and University of California, Berkeley, California 94720, USA*
[47] *California State University, Fresno, California 93740, USA*
[48] *University of California, Riverside, California 92521, USA*
[49] *Florida State University, Tallahassee, Florida 32306, USA*
[50] *Fermi National Accelerator Laboratory, Batavia, Illinois 60510, USA*
[51] *University of Illinois at Chicago, Chicago, Illinois 60607, USA*
[52] *Northern Illinois University, DeKalb, Illinois 60115, USA*
[53] *Northwestern University, Evanston, Illinois 60208, USA*
[54] *Indiana University, Bloomington, Indiana 47405, USA*
[55] *University of Notre Dame, Notre Dame, Indiana 46556, USA*
[56] *Purdue University Calumet, Hammond, Indiana 46323, USA*
[57] *Iowa State University, Ames, Iowa 50011, USA*
[58] *University of Kansas, Lawrence, Kansas 66045, USA*
[59] *Kansas State University, Manhattan, Kansas 66506, USA*
[60] *Louisiana Tech University, Ruston, Louisiana 71272, USA*
[61] *University of Maryland, College Park, Maryland 20742, USA*
[62] *Boston University, Boston, Massachusetts 02215, USA*
[63] *Northeastern University, Boston, Massachusetts 02115, USA*
[64] *University of Michigan, Ann Arbor, Michigan 48109, USA*
[65] *Michigan State University, East Lansing, Michigan 48824, USA*
[66] *University of Mississippi, University, Mississippi 38677, USA*
[67] *University of Nebraska, Lincoln, Nebraska 68588, USA*
[68] *Princeton University, Princeton, New Jersey 08544, USA*
[69] *State University of New York, Buffalo, New York 14260, USA*
[70] *Columbia University, New York, New York 10027, USA*
[71] *University of Rochester, Rochester, New York 14627, USA*
[72] *State University of New York, Stony Brook, New York 11794, USA*
[73] *Brookhaven National Laboratory, Upton, New York 11973, USA*
[74] *Langston University, Langston, Oklahoma 73050, USA*
[75] *University of Oklahoma, Norman, Oklahoma 73019, USA*
[76] *Oklahoma State University, Stillwater, Oklahoma 74078, USA*
[77] *Brown University, Providence, Rhode Island 02912, USA*
[78] *University of Texas, Arlington, Texas 76019, USA*
[79] *Southern Methodist University, Dallas, Texas 75275, USA*
[80] *Rice University, Houston, Texas 77005, USA*
[81] *University of Virginia, Charlottesville, Virginia 22901, USA*
[82] *University of Washington, Seattle, Washington 98195, USA*

(Dated: Dec 5, 2006)

We search for the technicolor process $p\overline{p} \to \rho_T/\omega_T \to W\pi_T$ in events containing one electron and two jets, in data corresponding to an integrated luminosity of 390 pb^{-1}, recorded by the D0 experiment at the Fermilab Tevatron. Technicolor predicts that technipions, π_T, decay dominantly into $b\overline{b}$, $b\overline{c}$, or $\overline{b}c$, depending on their charge. In these events b and c quarks are identified by their secondary decay vertices within jets. Two analysis methods based on topological variables are

presented. Since no excess above the standard model prediction was found, the result is presented as an exclusion in the π_T vs. ρ_T mass plane for a given set of model parameters.

PACS numbers: 12.60.Nz, 13.85.Rm

Technicolor (TC), first formulated by Weinberg and Susskind [1, 2], provides a dynamical explanation of electroweak symmetry breaking through a new strong $SU(N_{TC})$ gauge interaction acting on new fermions, called "technifermions." Technicolor is a non-Abelian gauge theory modeled after Quantum Chromodynamics (QCD). In its low-energy limit, a spontaneous breaking of the global chiral symmetry in the technifermion sector leads to electroweak symmetry breaking. The Nambu-Goldstone bosons produced in this process are called technipions, π_T, in analogy with the pions of QCD. Three of these technipions become the longitudinal components of the W and Z bosons, making them massive.

An additional gauge interaction, called extended technicolor [3, 4], couples standard model fermions and technifermions to provide a mechanism for generating quark and lepton masses. By limiting the running of the technicolor coupling constant, walking technicolor [5] avoids flavor-changing neutral currents. To generate masses as large as the top quark mass, another interaction, topcolor, seems to be necessary, thereby giving rise to topcolor-assisted technicolor models [6].

Extensions of the basic technicolor model tend to require the number N_D of technifermion doublets to be large. In general, the technicolor scale $\Lambda_{TC} \approx O(1) \times F_{TC}$, where F_{TC} is the technipion decay constant, depends inversely on the number of technifermion doublets: $F_{TC} \approx 246\,\mathrm{GeV}/\sqrt{N_D}$. For large N_D, the lowest lying technihadrons have masses on the order of few hundred GeV. This scenario is referred to as low-scale technicolor [7]. Low-scale technicolor models predict the existence of scalar technimesons, $\pi_T^{\pm}$ and π_T^0, and vector technimesons, ρ_T and ω_T. General features of low-scale technicolor have been summarized in the technicolor strawman model (TCSM) [8, 9]. The analysis presented in this paper is based on Ref. [9].

Vector technimesons are expected to be produced with substantial rates at the Fermilab Tevatron Collider via the Drell-Yan-like electroweak process $p\overline{p} \to \rho_T + X$ or $\omega_T + X$. In walking technicolor, it is expected that vector technimesons decay to a gauge boson (γ, W, Z) and a technipion or to fermion-antifermion pairs. The production cross sections and branching fractions depend on the masses of the vector technimesons, $M(\rho_T)$ and $M(\omega_T)$, on the technicolor-charges of the technifermions, on the mass differences between the vector and scalar technimesons, which determine the spectrum of accessible decay channels, and on two mass parameters, M_A for axial-vector and M_V for vector couplings. The parameter M_V controls the rate for the decay $\rho_T, \omega_T \to \gamma + \pi_T$ and is unknown *a priori*. Scaling from the QCD decay $\rho, \omega \to \gamma + \pi^0$, the authors of Ref. [9] suggest a value of several hundred GeV. We set $M_A = M_V$, and evaluate the production and decay rates at two different values: 100 and 500 GeV. For all other parameters, we use the default values quoted in Table III of Ref. [9]. Technipion coupling to the standard model particles is proportional to their masses, therefore technipions in the mass range considered here predominantly decay into $b\bar{b}$, $b\bar{c}$, or $\bar{b}c$, depending on their charge.

In this Letter, we describe a search for the decay of vector technimesons to $W\pi_T$, followed by the decays $W \to e\nu$ and $\pi_T \to b\bar{b}$, $b\bar{c}$, or $c\bar{b}$. In the D0 detector, which is described in detail in Ref. [10], the signature of this process is an isolated electron and missing transverse momentum ($\not\!\!p_T$) from the undetected neutrino from the decay of the W boson, and two jets of hadrons coming from the fragmentation of the quarks from the decay of the technipion. Jets are reconstructed using the Run II cone algorithm [11] with a cone size of 0.5. We search for events with this signature in the data collected with a single electron trigger until July 2004 and corresponding to an integrated luminosity of 388 ± 25 pb^{-1} [12].

There are a number of standard model processes that can result in the same final state signature as $W\pi_T$ production. Vector boson production in association with jets is the dominant background. Z boson production can be suppressed by vetoing on a second electron and requiring significant $\not\!\!p_T$. Most of the jets in W+jets events originate from the fragmentation of light quarks or gluons and therefore requiring the explicit identification of at least one jet from the fragmentation of a b or c quark suppresses most of this background, leaving only $W + b\bar{b}$, $W + b$, $W + c\bar{c}$, and $W + c$ events. Top quark production followed by the decay to $e\nu b$ is another background. Top-antitop quark pair production typically results in either an additional lepton or a higher jet multiplicity from the decay of the second top quark, and this background can be reduced by selecting events with exactly two jets. Single top quark production is an irreducible background, but it has a smaller cross section. We simulate all these processes using either PYTHIA [13] or ALPGEN [14] Monte Carlo (MC) generators, followed by the D0 detector simulation based on GEANT [15]. Quark hadronization and fragmentation is simulated using PYTHIA.

The multijet background is due to events with poorly measured jets, resulting in missing momentum and a jet that is misidentified as an electron. Background from the mistagged W+jets process originates from events in which a light-quark or gluon jet is incorrectly identified as a b jet. These instrumental background contributions are estimated from the same data sample before requiring

the identification of a b jet.

We select events in which there is exactly one well-identified electron based on tracking and calorimeter data with transverse momentum $p_T > 20$ GeV and pseudo-rapidity $|\eta| < 1.1$ [16]. There must be significant $\not\!\!p_T$, measured in two ways: $\not\!\!p_T^{\rm obj} > 20$ GeV computed as the negative sum of the jet momentum vectors and the electron momentum vector and $\not\!\!p_T > 20$ GeV which also includes the calorimeter energy deposit not assigned to the electron or the jets. We require the transverse mass $M_T(e\nu) > 30$ GeV. We further require the presence of exactly two jets with $p_T > 20$ GeV and $|\eta| < 2.5$.

To further reduce backgrounds, we take advantage of the long lifetime of b flavored hadrons. Tracks from the decay products of b hadrons may not project back to the proton-antiproton collision, but have a significant impact parameter. They can therefore be identified and used to reconstruct the decay vertex of the b hadron. A jet is tagged as a b jet if there is a secondary decay vertex within $\Delta\mathcal{R} = \sqrt{(\Delta\eta)^2 + (\Delta\phi)^2} < 0.5$ of the jet axis. We require at least one of the jets to be b-tagged. This leaves us with 117 events in our final data sample.

The expected background event yields are listed in Table I. When estimating these yields, each Monte Carlo event is weighted by the probability that at least one jet is tagged as a b jet. The tagging probability is parameterized as a function of jet flavor, jet p_T, and η. The efficiency of tagging a jet from the fragmentation of a b quark is derived from collider data which were enriched in their b jet contents by requiring a muon to be reconstructed within at least one jet to preferentially select jets with semileptonic b decays. The probability of tagging a c jet is derived from the tagging probability for b jets by multiplying by the ratio of tagging probabilities for c and b jets derived from MC simulations. We derive the probability to tag a light-quark or gluon jet from a set of dijet events, corrected for contamination by c and b jets. The Monte Carlo events are also weighted by the ratios of jet and electron finding efficiencies in Monte Carlo and collider data. Electron finding efficiencies are measured in $Z \to ee$ events in both data and Monte Carlo.

We use the PYTHIA event generator to simulate signal events, modeling initial state and final state radiation, fragmentation, and hadronization. To generate $W\pi_T$ signal events for a range of values of the technimeson masses, we use a fast, parameterized detector simulation that was tuned to reproduce the kinematic distributions and acceptances from events simulated with the detailed GEANT-based detector simulation. For the cross section calculations, CTEQ5L [17] parton distribution functions are used. Finally, as is appropriate for this Drell-Yan-like process, the cross section is multiplied by a K-factor of 1.3 to approximate NLO contributions to the cross section [18]. We generate events with ρ_T masses from 160 GeV to 220 GeV and assume $M(\omega_T) = M(\rho_T)$. The π_T mass values start at the kinematic threshold for $W\pi_T$ production at $M(\pi_T) = M(\rho_T) - M(W)$ and go down to $M(\pi_T) = M(\rho_T)/2 - 5$ GeV where the decay channel $\rho_T^{\pm(0)} \to \pi_T^{\pm(0,\pm)}\pi_T^{0(0,\mp)}$ is accessible, reducing the branching fraction of $\rho_T^{\pm(0)} \to W\pi_T$.

TABLE I: Number of events observed in the data and expected from signal and background sources after the kinematic selection; only statistical errors are reported. For the expected number of signal events quoted we assume $M(\rho_T) =$ 210 GeV and $M(\pi_T) = 110$ GeV.

Final data sample	117
Signal:	
$\rho_T/\omega_T \to W + \pi_T \to e\nu b\overline{b}$ ($M_V = 100$ GeV)	11.1 ± 0.1
$\rho_T/\omega_T \to W + \pi_T \to e\nu b\overline{b}$ ($M_V = 500$ GeV)	17.1 ± 0.2
Physics background:	
$t\overline{t} \to \ell\nu bq\overline{q}\overline{b}$	7.9 ± 0.5
$t\overline{t} \to \ell^+\nu b\ell^-\nu\overline{b}$	14.1 ± 0.3
$W^* \to tb \to e\nu b\overline{b}$ or $\tau\nu b\overline{b}$	3.5 ± 0.1
$tqb \to e\nu b\overline{b}$ or $\tau\nu b\overline{b}$	4.3 ± 0.1
$W(\to e\nu)$ + heavy flavor	56.4 ± 4.2
$WZ \to e\nu b\overline{b}$	1.10 ± 0.02
$Z(\to e^+e^-)$	0.5 ± 0.4
$Z(\to e^+e^-) + b\overline{b}$	0.60 ± 0.03
Instrumental background:	
multijet events	16.3 ± 3.2
mistagged $W(\to e\nu)$ + jets	10.3 ± 0.3
Total background	115.1 ± 5.4

At this point our data sample is still dominated by background. We therefore use additional variables that characterize the topology of the events to discriminate between signal and background. These variables are the azimuthal angle difference between the two jets $\Delta\phi(j,j)$, the azimuthal angle difference between the electron and the $\not\!\!p_T$, $\Delta\phi(e,\not\!\!p_T)$, the transverse momentum of the dijet system $p_T(jj)$, the scalar sum of the transverse momenta of the electron and the two jets H_T^e, the invariant mass of the dijet system $M(jj)$, and the invariant mass of the W boson-dijet system $M(Wjj)$. The technicolor particles are expected to have narrow widths (≈ 1 GeV). We should therefore see enhancements in the distributions of $M(jj)$ and $M(Wjj)$, consistent in width with the detector resolution. $M(jj)$ corresponds to the reconstructed π_T mass and $M(Wjj)$ corresponds to the reconstructed ρ_T mass. We reconstruct the W boson from the electron and the missing transverse momentum using the W boson mass constraint to solve for p_z of the neutrino. If there are two real solutions, we take the smaller value of neutrino $|p_z|$. If there is only a complex solution, we take the real part. Distributions of these variables are shown in Figs. 1 and 2. We use two approaches to separate signal and background, a cut-based analysis and a neural network analysis.

The cut-based analysis is optimized using Monte Carlo simulations to maximize the ratio $S/\sqrt{B}$ for every set of technimeson mass values. S is the expected number of

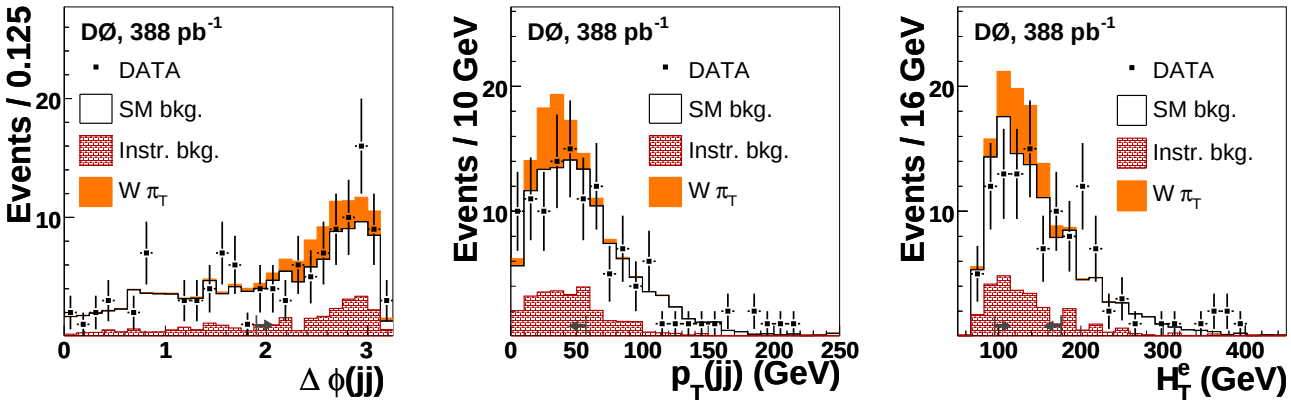

FIG. 1: Distributions of $\Delta\phi(jj)$, $p_T(jj)$ and H_T^e after final kinematic selection. The $W\pi_T$ signal is shown for $M(\rho_T) = 210$ GeV and $M(\pi_T) = 110$ GeV. Arrows at the bottom indicate the cuts applied in the cut-based analysis for the signal mass point shown.

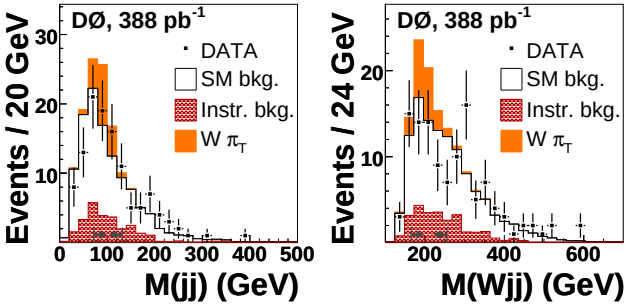

FIG. 2: Distributions of $M(jj)$ and $M(Wjj)$ after final kinematic selection. The $W\pi_T$ signal is shown for $M(\rho_T) = 210$ GeV and $M(\pi_T) = 110$ GeV. Arrows at the bottom indicate the cuts applied in the cut-based analysis for the signal mass point shown.

$W\pi_T$ events and B is the expected number of background events. For each topological variable, the $S/\sqrt{B}$ ratio is evaluated as a function of the value of the variable to determine a set of lower, upper, or window cuts which maximizes this ratio.

The neural network analysis uses the topological variables H_T^e, $\Delta\phi(e, \not{p}_T)$, $\Delta\phi(jj)$, $p_T(jj)$, the transverse momenta of both jets and of the electron and $\not{p}_T$. A two-stage neural network based on the Multi Layer Perceptron algorithm [19] is used. The first stage consists of three independent networks which are trained to reject the three main backgrounds, top quark production, $W + b\bar{b}$ production, and all other W+jets production including heavy flavors. Each of these three networks has eight input nodes and one hidden layer with 24 nodes. The second stage network has three input nodes, connected to the outputs of the three networks in the first stage, and one hidden layer with six nodes. The second stage network is trained using all nine physics background processes. The networks are trained separately for each set of technicolor mass values. We then apply the trained neural networks to the collider data, technicolor signals, and physics and instrumental backgrounds to obtain the discriminator output spectra. We optimize the discriminator cut for every set of techniparticle masses to maximize $S/\sqrt{B}$.

There is no excess in our data over the expected background. We compute upper limits on the $\rho_T \to W\pi_T \to e\nu\ b\bar{b}(\bar{c})$ production cross section times branching fraction. In the cut-based analysis, which is a simple counting experiment, we compute an upper 95% C.L. limit on the signal using Bayesian statistics [20]. The neural network analysis performs a maximum likelihood fit of the data in the $M(\rho_T), M(\pi_T)$ plane to signal and background expectations. The backgrounds are constrained to their expected values within statistical and systematic uncertainties. The uncertainties in the background event yields total to 10–12% and the uncertainty in the signal selection efficiency is 10% for the cut-based analysis and 20% for the neural-net based analysis. The largest contributions to the systematic uncertainties are due to jet reconstruction efficiency, jet energy scale, b-tagging efficiency, and, only for the signal, from the difference between fast and fully simulated detector Monte Carlo. The 95% C.L. upper limit on the signal cross section is then determined by the number of signal events below which lies 95% of the integral over the resulting likelihood function.

The expected sensitivity and the regions excluded at 95% C.L. by both analyses in the $M(\rho_T), M(\pi_T)$ plane for $M_V = 500$ GeV are shown in Fig. 3. For $M_V = 100$ GeV, only a small region around $M(\rho_T) = 190$ GeV and $M(\pi_T) = 95$ GeV can be excluded. We note from Fig. 3(a), that the expected sensitivity of the neural network analysis is better than that of the cut-based analysis, as indicated by the larger 95% C.L. exclusion region.

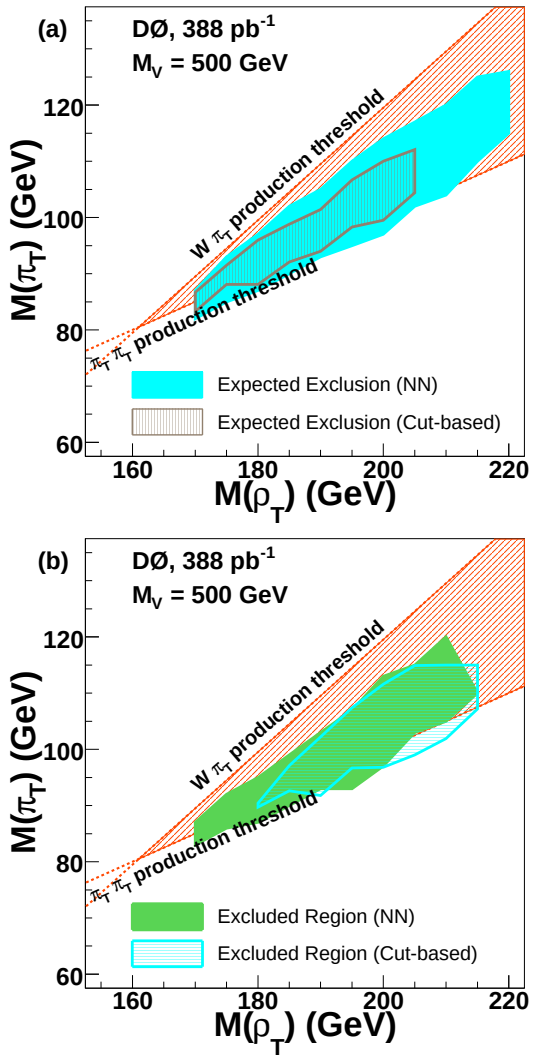

FIG. 3: Expected region of exclusion (a) and excluded region (b) at the 95% C.L. in the $M(\rho_T), M(\pi_T)$ plane for $\rho_T \to W\pi_T \to e\nu\, b\bar{b}(\bar{c})$ production with $M_V = 500$ GeV. Kinematic thresholds from $W\pi_T$ and $\pi_T\pi_T$ are shown on the figures.

We quote the observed 95% C.L. exclusion region in the $M(\rho_T), M(\pi_T)$ plane in Fig. 3(b) by the neural network analysis as our measurement [21].

The results presented in this paper cannot be compared directly to those previously published [23]. The CDF experiment did not use Ref. [8] and [9], but rather the models described in the earlier paper of Ref. [7], a precursor to the TCSM. The LEP experiments used Ref. [8] in which the cross sections, while appropriate for narrow ρ_T production in $\bar{q}q$ collisions, are incorrect for off-resonance production in e^+e^- collisions such as at LEP (see Ref. [24]). Although differences in the employed TC models preclude a direct comparison with previous searches, the current search achieves a higher sensitivity to the considered physics process.

We thank Ken Lane for helpful discussions, the staffs at Fermilab and collaborating institutions, and acknowledge support from the DOE and NSF (USA); CEA and CNRS/IN2P3 (France); FASI, Rosatom and RFBR (Russia); CAPES, CNPq, FAPERJ, FAPESP and FUNDUNESP (Brazil); DAE and DST (India); Colciencias (Colombia); CONACyT (Mexico); KRF and KOSEF (Korea); CONICET and UBACyT (Argentina); FOM (The Netherlands); PPARC (United Kingdom); MSMT (Czech Republic); CRC Program, CFI, NSERC and WestGrid Project (Canada); BMBF and DFG (Germany); SFI (Ireland); The Swedish Research Council (Sweden); Research Corporation; Alexander von Humboldt Foundation; and the Marie Curie Program.

[*] On leave from IEP SAS Kosice, Slovakia.
[†] Visitor from Helsinki Institute of Physics, Helsinki, Finland.

[1] S. Weinberg, Phys. Rev. D **13**, 974 (1976).
[2] L. Susskind, Phys. Rev. D **20**, 2619 (1979).
[3] S. Dimopoulos and L. Susskind, Nucl. Phys. **B155**, 237 (1979).
[4] E. Eichten and K. Lane, Phys. Lett. **90B**, 125 (1980).
[5] B. Holdom, Phys. Rev. D **24**, 1441 (1981). Phys. Lett. **150B**, 301 (1985). T. Appelquist, D. Karabali, and L. C. R. Wijewardhana, Phys. Rev. Lett. **57**, 957 (1986).
[6] C. T. Hill, Phys. Lett. B **345**, 483 (1995).
[7] K. Lane and E. Eichten, Phys. Lett. B **222**, 274 (1989).
[8] K. Lane, Phys. Rev. D**60**, 075007 (1999).
[9] K. Lane and S. Mrenna, Phys. Rev. D**67**, 115011 (2003).
[10] DØ Collaboration, V.M. Abazov, *et al.*, Nucl. Instrum. and Methods A **565**, 463 (2006).
[11] G. Blazey *et al.*, in *Proceedings of the Workshop: "QCD and Weak Boson Physics in Run II,"* edited by U. Baur, R.K. Ellis and D. Zeppenfeld (Fermilab, Batavia, IL, 2000), p.47; see Sec. 3.5 for details.
[12] T. Edwards *et al.*, FERMILAB-TM-2278-E (2004).
[13] T. Sjöstrand *et al.*, Comput. Phys. Commun. **135**, 238 (2001). We use PYTHIA version 6.224.
[14] F. Caravaglios, M. L. Mangano, M. Moretti and R. Pittau, Nucl. Phys. **B 539** 215 (1999).
[15] R. Brun and F. Carminati, CERN Program Library Long Writeup W5013, 1993 (unpublished).
[16] $\eta = -\ln[\tan(\theta/2)]$ and θ is the polar angle with respect to the proton beam direction.
[17] H. L. Lai, *et al.*, Eur. Phys. J. C **12**, 375 (2000).
[18] R. Hamberg, W. L. Van Neerven, and T. Matsura, Nucl. Phys. **B359**, 343 (1991).
[19] `http://schwind.home.cern.ch/schwind/MLPfit.html`
[20] I. Bertram *et al.*, FERMILAB-TM-2104 (2000).
[21] Consistent scaling of luminosity and background prior to optimization, using the new D0 luminosity [22] will lead to somewhat better limits. Nevertheless, we choose to keep the analysis consistent with the previous estimate of the luminosity value [12].
[22] T. Andeen *et. al.*, FERMILAB-TM-2365-E (2006), in preparation.
[23] CDF Collaboration, T. Affolder *et al.*, Phys. Rev. Lett.

84, 1110 (2000); DELPHI Collaboration, J. Abdallah *et al.*, Eur. Phys. J. C **22**, 17 (2001).
[24] K. Lane, Lectures at Frascati Spring School, *Technicolor 2000*, Frascati, Rome, Italy, 2000; hep-ph/0007304.